Manifestation of sulfur-to-sulfur interaction in complexes of iron, ruthenium and osmium

Icaro de Sousa Moreira [a], Joacy Batista de Lima [b],
Douglas Wagner Franco [c,*]

[a] *Universidade Federal do Ceará, Departamento de Química Orgânica e Inorgânica,
Fortaleza CE, Brazil*
[b] *Universidade Federal do Maranhão, Centro Tecnológico, Departamento de Química,
São Luís MA, Brazil*
[c] *Instituto de Química de São Carlos/USP,
Departamento de Química e Física Molecular. Cx. Postal 780, 13560-970 São Carlos SP, Brazil*

This paper is dedicated to our colleague and friend Professor Eduardo Stadler in memoriam.

Contents

Abstract

The electron conducting ability of the –S–S– bridge was investigated using iron, ruthenium and osmium as metal centers and the bridging ligands 4,4′-dithiodipyridine and bis(4-

* Corresponding author. Tel.: + 55-16-272-3813; fax: + 55-16-273-9982.
  E-mail address: douglas@iqsc.sc.usp.br (D. Wagner Franco)

pyridine)sulfide. The observed back-bonding manifestations in mononuclear complexes, (evaluated through pK_a, MLCT and $E°_{1/2}$ data), the calculated comproportionation constant (K_c) for the homobinuclear species and the near-infrared (NIR) band characteristics of the homobinuclear and heterobinuclear mixed valence complexes consistently indicate a strong electron delocalization through the disulfide bridge. The available data strongly suggest a correlation between the conducting efficiency of the –S–S– bridge and the existence of a multiply bonded L···S···S···L core. © 2000 Elsevier Science S.A. All rights reserved.

Nomenclature

BPMS	bis(4-pyridilmethyl)disulfide
DPS	bis(4-pyridyl)sulfide
DTDP	4,4′-dithiodipyridine
2,2′-DTDP	2,2′-dithiodipyridine
4,4′-bpy	4,4′-bipyridine
spy$^-$	2-mercaptopyridine anion
pz	pyrazine
isn	isonicotinamide
py	pyridine
'S'$_4^{-2}$	1,2-bis(2-mercaptophenyl)thioethane(2$^-$)
PPh$_3$	triphenyl phosphine
P(Ome)$_3$	trimethyl phosphite

1. Introduction

Ruthenium(II,III) ammines are inert to ligand substitution due to the metal center configuration (d^6 and d^5, low spin) [1,2] but are quite reactive regarding electron transfer reactions. The inertness of these complexes is such that under appropriate conditions the coordination sphere remains intact after the electron transfer. These characteristics allow one to investigate changes in the ligands and in the metal center properties as a function of the metal center oxidation state [1,2].

Using ruthenium ammines as a model, Taube [3–16] and co-workers have devoted much effort to develop the synthetic and the reactivity aspects of sulfur containing ligands. They were able to isolate the first well characterized [3] H$_2$S complex with a transition metal ion and the first ruthenium disulfide [4], recognize

the availability of the $3d_\pi$ sulfur orbitals for electron delocalization between the two metal centers and, investigating ligands containing sulfur atoms, lying apart from each other, described remarkable examples of sulfur-to-sulfur through space interactions [9–13]. Recently the same Laboratory reported S–C bound cleavage activation by Ru(III) [14].
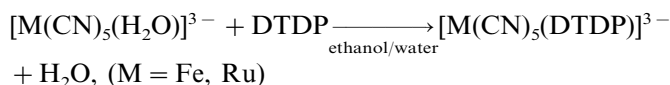
Inspired by these earlier studies [3–16], we decided to study the abilities of the –S–S– bridge as an electron conductor. Despite the well known relevance of the sulfur–sulfur interaction in biological processes [17], molecular electronics [18], catalysis [19], superconductors [20] and energy storage technologies [21], little is known about electron delocalization along the –S–S– bridge.

Extending Taube's work we chose dithiodipyridines as bridging ligands and ruthenium, iron and osmium complexes, whose core structures are resistant to ligand substitution, to start investigation of the –S–S– unity as an electron conductor. Despite the well known oxidative addition reaction of disulfides to metal centers, our first experiments with the 4,4'-dithiodipyridine ligand allowed us to isolate stable complexes of ruthenium ammines, pentacyanoiron and pentacyanoruthenate. Besides the ability of the –S–S– bridge to conduct electrons, it was possible to observe a noticeable gain in the sulfur–sulfur bond stability with respect to reduction, when at least one of the pyridine rings was coordinated to the ruthenium or iron center. This gain in stability was not observed when the parent molecule 2,2'-dithiodipyridine was used. In this case the –S–S– bond was easily activated by the 18-electron metal center containing only one dissociable ligand.
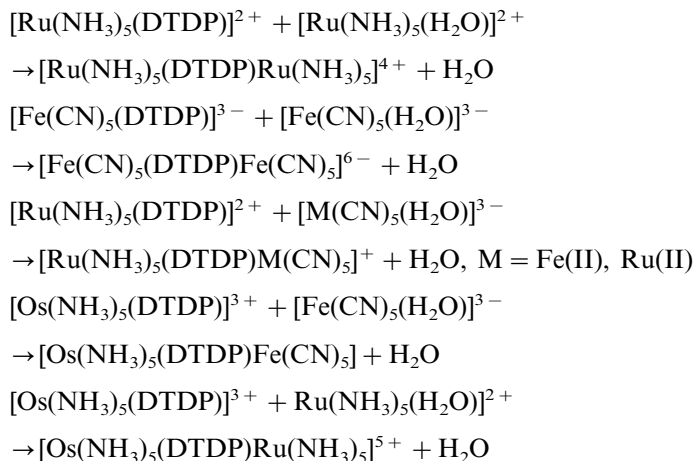
In our approach, the effects of the nature of the sulfur spacer, the nature of the metal center and the distance between the metal centers in the electron delocalization were investigated.
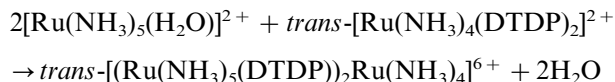
2. Synthesis of the complexes

The mononuclear species were obtained [22–29] by reacting the aquo species $[Ru(CN)_5(H_2O)]^{3-}$ and $[Fe(CN)_5(H_2O)]^{3-}$ with the 4,4'-dithiodipyridine (DTDP):

$$[M(CN)_5(H_2O)]^{3-} + DTDP \xrightarrow[\text{ethanol/water}]{} [M(CN)_5(DTDP)]^{3-}$$
$$+ H_2O, \ (M = Fe, \ Ru)$$

$$[M(NH_3)_5(H_2O)]^{3+/2+} + DTDP \xrightarrow[\text{acetone}]{} [M(NH_3)_5(DTDP)]^{3+/2+}$$
$$+ H_2O, \ (M = Ru, \ Os)$$

$$\textit{trans-}[Ru(NH_3)_4(H_2O)_2]^{2+} + 2DTDP \xrightarrow[\text{acetone}]{} \textit{trans-}[Ru(NH_3)_4(DTDP)_2]^{2+}$$

The aquo species $[Ru(CN)_5(H_2O)]^{3-}$ and $Fe(CN)_5(H_2O)]^{3-}$ were generated in solution. The binuclear complexes were synthesized by [22,23,27,29] reacting $[Ru(NH_3)_5DTDP]^{2+}$, $[Os(NH_3)_5DTDP]^{3+}$ and $[Fe(CN)_5DTDP]^{3-}$ with the desired aquo species: $[Ru(NH_3)_5(H_2O)]^{2+}$, $[Os(NH_3)_5(H_2O)]^{3+}$, $[Ru(CN)_5(H_2O)]^{3-}$ and $[Fe(CN)_5(H_2O)]^{3-}$ in aqueous medium:

$$[Ru(NH_3)_5(DTDP)]^{2+} + [Ru(NH_3)_5(H_2O)]^{2+}$$

$$\rightarrow [Ru(NH_3)_5(DTDP)Ru(NH_3)_5]^{4+} + H_2O$$

$$[Fe(CN)_5(DTDP)]^{3-} + [Fe(CN)_5(H_2O)]^{3-}$$

$$\rightarrow [Fe(CN)_5(DTDP)Fe(CN)_5]^{6-} + H_2O$$

$$[Ru(NH_3)_5(DTDP)]^{2+} + [M(CN)_5(H_2O)]^{3-}$$

$$\rightarrow [Ru(NH_3)_5(DTDP)M(CN)_5]^{+} + H_2O, \ M = Fe(II), \ Ru(II)$$

$$[Os(NH_3)_5(DTDP)]^{3+} + [Fe(CN)_5(H_2O)]^{3-}$$

$$\rightarrow [Os(NH_3)_5(DTDP)Fe(CN)_5] + H_2O$$

$$[Os(NH_3)_5(DTDP)]^{3+} + Ru(NH_3)_5(H_2O)]^{2+}$$

$$\rightarrow [Os(NH_3)_5(DTDP)Ru(NH_3)_5]^{5+} + H_2O$$

The trinuclear complex $[(Ru(NH_3)_5(DTDP))_2Ru(NH_3)_4]^{6+}$ was generated [28] by two independent reactions:

$$2[Ru(NH_3)_5(H_2O)]^{2+} + trans\text{-}[Ru(NH_3)_4(DTDP)_2]^{2+}$$

$$\rightarrow trans\text{-}[(Ru(NH_3)_5(DTDP))_2Ru(NH_3)_4]^{6+} + 2H_2O$$

and

$$2[Ru(NH_3)_5(DTDP)]^{2+} + trans\text{-}[Ru(NH_3)_4(H_2O)_2]^{2+}$$
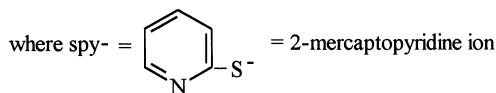
$$\rightarrow [(Ru(NH_3)_5(DTDP))_2Ru(NH_3)_4]^{6+} + H_2O$$
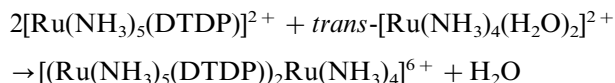
These compounds were isolated and characterized [22–30] by microanalysis, spectroscopic (UV–vis, IR, Mössbauer, NMR and ESR spectroscopies) and voltammetric techniques (CV, DPP).

The attempts to isolate the binuclear complexes $[Os(NH_3)_5(DTDP)Os(NH_3)_5]X_6$ and $Na_6[Ru(CN)_5(DTDP)Ru(CN)_5]$ have proven so far to be unsuccessful [29].

In contrast with the observed data for 4,4′-dithiodipyridine-$[Ru(NH_3)_5(H_2O)]^{2+}$ system, it was not possible to isolate the 2,2′-dithiodipyridine (2,2′-DTDP) ruthenium complex by reacting this ligand with the aquopentaammine species. Oxidative addition of the disulfide to the metal center was observed with –S–S– bridge cleavage and the metal center oxidation [31]:

$$2[Ru^{II}(NH_3)_5(H_2O)]^{2+} + 2,2'\text{-}DTDP \xrightarrow[\text{acetone}]{k_1} 2[Ru^{III}(NH_3)_5(spy)]^{2+}$$

where spy- = –S⁻ = 2-mercaptopyridine ion

The pentaammine-2-mercaptopyridine complex is formed with a second order specific rate constant $k_1 = 0.3 \ M^{-1} \ s^{-1}$, at 25°C. Since pyridine replaces H_2O [31] in $[Ru(NH_3)_5(H_2O)]^{2+}$ at $k_1 = 0.0093 \ M^{-1} \ s^{-1}$, the possibility of 2,2′-DTDP

coordination to the Ru(II) center followed by a intramolecular electron transfer process was proposed [32].

3. Mononuclear complexes, characterization and properties

3.1. Electron spin resonance

Electron paramagnetic resonance is of particular interest in the analysis of low spin d^5 osmium and ruthenium ammines [25,33,34]. The energy level of these systems can be described as an orbital triplet ground state t_{2g} and the highest lying orbital doublet e_g. In these complexes (d^5, strong field) the ground state configuration will be $t_{2g}^5 e_g^0$ and the presence of an axial distortion Δ will split the orbital triplet into a singlet (d_{xy}) and a doublet (d_{xz}, d_{yz}), which can undergo a further split by a rhombic distortion V to the regular octahedron. The effect of the ligand field and spin orbit coupling on the energy levels for these systems has already been examined [25,33,34] and since the spin-orbit parameter λ is quite large, it is difficult to describe rigorously the ground state in terms of pure d_{xy}, d_{xz} and d_{yz} orbitals.

In the angular overlap model (AOM) treatment [25,33,34] of MX_5Y and the *trans*-MX_4XZ, ($Y = Z$ or $Y \neq Z$) complexes, the $d(t_{2g})$ orbitals, which have unpaired electrons, were recognized to interact with the ligands in a π fashion.

In the AOM symbolism [25,34], the tetragonal distortion Δ in the ammine species, when $V = 0$, will be:

$$\Delta = [\varepsilon_\pi(X) - \varepsilon_\pi(Y)] \text{ for } MX_5Y$$

and

$$\Delta = [2\varepsilon_\pi(X) - 2\varepsilon_\pi(Y)] \text{ for } MX_4Y_2$$

where $X = NH_3$ and ε_π is the energy of interaction for the antibonding d orbitals with one ligand atom. Assuming that ε_π for $NH_3 \approx 0$, which is quite reasonable since the ammonia ligand has no π electrons to donate, $\varepsilon_\pi(Y)$ can be calculated from the Δ values.

In this model, (see Table 1), the positive value of Δ, and therefore of ε_π, will reflect the better π donation ability of Y with reference to NH_3. Thus, the negative sign for ε_π (DTDP) would be an indication of the Os(III) back-bonding into the π^* orbital of the pyridine ring. This behavior is not completely unexpected since conversely to Ru(III), which is well known not to be able to back-bond, Os(III) is reported to act as a π donor in $[Os(NH_3)_5pz]^{3+}$ complex [35–37]. Fig. 1 shows as illustration [25] the powder EPR spectrum of $[Os(NH_3)_5(DTDP)](CF_3SO_3)_3$.

3.2. Ligand's acid–base properties

The measured changes in the ligand's acid–base properties (pK_a values), induced by coordination to a metal center, have been extensively used to understand how the π and σ components of the metal–ligand bond change with changes in the metal center oxidation state [38–42].

As observed in Table 2, the coordination of DTDP and pz to Os(II) and Ru(II) centers leads to an increase in the coordinated ligand basicity. This effect was recognized as a manifestation of M(II) → L back-bonding, which for the ammines is stronger for Os(II) than for Ru(II). Thus, the observed increase in ligand basicity is 0.7 and 6.8 pK_a units for DTDP and pz, respectively, when coordinated to Os(II), whereas, when the coordination center is Ru(II), the ΔpK_a values are 0.4 and 1.9, respectively.

The changes observed follow the same trend for both pz and DTDP ligands but the effects observed for the pyrazine systems are larger than those for the DTDP

Table 1

Experimental g values[a] and ligand field parameters for ruthenium and osmium complexes

Species[b]	g_1	g_2	g_3	Δ/λ[d]	V (cm^{-1})[e]	ε_π	Ref.
$[Ru(NH_3)_5(H_2O)]^{3+}$	2.64	[c]		0.18	0.00	180	[25,33]
$[Ru(NH_3)_5(DTDP)]^{3+}$	2.29	1.91		0.15	0.00	150	[25]
trans-$[Ru(NH_3)_4(DTDP)_2]^{3+}$	2.54	2.41	1.77	0.24	−0.05	120	[28,29]
$[Os(NH_3)_5(CF_3SO_3)]^{2+}$	2.12	1.90	1.61.	0.15	0.09	450	[25]
$[Os(NH_3)_5(H_2O)]^{3+}$	2.16	2.16	1.18	0.35	0.00	1050	[25]
$[Os(NH_3)_5(DTDP)]^{3+}$	1.71	1.71	2.23	−0.22	(0.00)	−660	[25]

[a] g values calculated using a homemade program written by Bruce R. McGarvey [33].
[b] $CF_3SO_3^-$ or PF_6^- salts.
[c] $0.6 \geq g_{//} \geq 0$.
[d] $\lambda \cong 1.000$ cm^{-1} for Ru(III) and 3000 cm^{-1} for Os(III), Δ = tetragonal distortion parameter.
[e] Rhombic parameter.
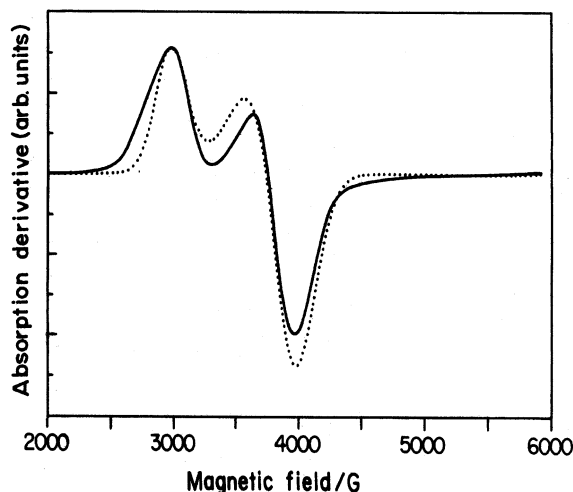
Fig. 1. Powder EPR spectrum [25] of $[Os(NH_3)_5DTDP](CF_3SO_3)_3$, 7K, $\nu = 9.30$ GHz.

Table 2
pK_a, pK_a^* and ΔpK_a data for coordinated and uncoordinated DTDP and pzH

Species	pK_a[a]	pK_a^{*}[b]	ΔpK_a[d]	Ref
$[Fe(CN)_5DTDPH]^{2-}$	4.4	7.2	2.8	[23]
$[Fe(CN)_5pzH^+]^{3-}$	1.5			[40]
$[Ru(CN)_5DTDPH]^{2-}$	4.7	6.7	2.0	[23]
$[Ru(CN)_5pzH]^{3-}$	1.9			[40]
$[Ru(NH_3)_5DTDPH]^{3+}$	5.2	6.8	1.6	[23]
$[Ru(NH_3)_5DTDPH]^{4+}$	3.2	1.9	−1.3	[23]
$[Ru(NH_3)_5pzH]^{4+}$	−0.8			[38]
$[Ru(NH_3)_5pzH]^{3+}$	2.5	7.3	4.8	[38]
$[Os(NH_3)_5pzH]^{3+}$	7.4			[39]
$[Os(NH_3)_5DTDPH]^{3+}$	5.5	nd[e]	nd[e]	[24,29]
$[Os(NH_3)_5DTDPH]^{4+}$	3.5	5.9	2.4	[24,29]
$DTDPH_2^{2+}$	2.7[c]			[43]
$DTDPH^+$	4.8[c]			[38]
pzH^+	0.6[c]			[24]

[a] For reaction $M^{III,II}$–$LH^+ + H_2O \leftrightarrows M^{II,III}$–$L + H_3O^+$
[b] $pK_a^* = pK_a + 2.86(v_1v_2)/2.3RT$, v_1 and v_2 are the MLCT frequencies for the deprotonated and the protonated forms [48].
[c] For the reaction $LH^+ + H_2O \leftrightarrows L + H_3O^+$ and $LH_2^{2+} + H_2O \rightarrow LH^+ + H_3O^+$, L = pz and DTDP
[d] $\Delta pK_a = pK_a^* - pK_a$.
[e] nd, data not available.

complexes. When comparing the π-bonding manifestation using pz and DTDP as probes, it should be emphasized that in $[Ru(NH_3)_5pzH]^{3+}$ the proton and the ligand coordination sites are both in the same ring. For $[Ru(NH_3)_5$-py-S–S-pyH$]^{3+}$ complex, the protonated nitrogen is in the second pyridine ring, which is separated, from the coordinated [43] one by about 8.2 Å, through the –S–S– bridge.

As described in the literature [40,41] for $[Ru(CN)_5pzH]^{2-}$ and $[Ru(CN)_5dmpzH]^{2-}$, no noticeable change has been observed [23] between the pK_a values of $[Ru(CN)_5DTDPH^+]^{2-}$ and $DTDPH^+$ acids. In these systems, the predominance of σ polarization effects over back-bonding in the Ru(II)–LH^+ bond still remains a matter of discussion.

For Os(III) and Ru(III) ammine complexes, where σ electronic effects are dominant, a decrease of 1.3 and 1.6 pK_a units was observed [23,24] in the coordinated ligand basicity with respect to the free $DTDPH^+$ acid [43,44]. This is consistent with the stronger Lewis acidic character of Ru(III) center relative to Os(III), which could be explained by the possibility of some Os(III) $\rightarrow$ L π interaction [25,35–37].

A comparison of ΔpK_a^* values, which is an indication [47–51] of the relative degree of the mixing between metal and ligand orbitals in the ground state [23,37,39,45–48], correlates with the analysis above, strongly suggesting an interaction between the two py rings in the DTDP complex.

3.3. Formal potential and charge transfer spectral data

The formal potentials $E^{\circ\prime}_{M(III)/M(II)}$ and the charge transfer band energy for the DTDP and DTDPH$^+$ metal complexes [22–29] follow the general trend observed for the similar species containing *N*-heterocycles ligands: py [39,41,45,52], pz [38,39,49], BPMS [53] and 4,4'-bpy [41,54], see Table 3. Both $E^{\circ\prime}_{M(III)/M(II)}$ and the energy for the MLCT bands exhibit a coherent behavior with that expected based on the π-bonding model [1,2,16].

Again, the protonation of the uncoordinated pyridine ring will provide information about the –S–S– bridge behavior. The –S–S– bridge acting as a good conductor would transform the DTDPH$^+$ ligand into a stronger π-acid than the DTDP, so a greater stabilization of the metal center's low oxidation state (II) relative to the (III) state would be expected upon DTDP protonation.

The observed shifts of $E^{\circ\prime}_{M(III)/M(II)}$ to more positive values and of λ_{MLCT} to lower energies with the coordinated DTDP protonation are therefore consistent with the conclusion that the disulphide bridge acts as a good conductor.

Table 3
Formal potentials and charge transfer spectral data for iron, ruthenium, osmium complexes

Species	$E^{\circ}_{M(III)/N(II)}$ [a]	λ_{MLCT}	λ_{LMCT}	$\varepsilon_{o(M^{-1}cm^{-1})}$	Ref.
[Fe(CN)$_5$(DTDP)]$^{3-}$	0.25	412	–	5.0×10^3	[23]
[Fe(CN)$_5$(DTDPH)]$^{2-}$		436	–	5.0×10^3	[23]
[Fe(CN)$_5$(BPMS)]$^{3-}$	0.22	394	–	4.1×10^3	[53]
[Fe(CN)$_5$(4,4'-bpy)]$^{3-}$		432			[55]
[Fe(CN)$_5$py]$^{3-}$	0.20	362			[33,41,46]
[HCN(CN)$_4$Fe(DTDPH)]$^-$		400		$\sim 10^3$	[23]
[Ru(CN)$_5$(DTDP)]$^{3-}$	0.71	348		6.0×10^3	[23]
[Ru(CN)$_5$(4,4'-bpy)]$^{3-}$		365			[41]
[Ru(CN)$_5$py]$^{3-}$	0.71	316			[41,45]
[Ru(CN)$_5$(DTDPH)]$^{2-}$		360		4.0×10^3	[23]
[Ru(NH$_3$)$_5$(DTDP)]$^{2+}$	0.095	458		6.6×10^3	[23]
[Ru(NH$_3$)$_5$(DTDPH)]$^{3+}$	0.14	474		1.4×10^4	[23]
trans-[Ru(NH$_3$)$_4$(DTDP)$_2$]$^{2+}$	0.31	460		1.3×10^4	[28,29]
[Ru(NH$_3$)$_5$(BPMS)]$^{2+}$	0.054	422		2.5×10^3	[53]
[Ru(NH$_3$)$_5$py]$^{2+}$	0.058	407		7.8×10^3	[41,52]
[Ru(NH$_3$)$_5$(4,4'-bpy)]$^{2+}$		475			[55]
[Os(NH$_3$)$_5$(DTDP)]$^{3+}$	−0.69	312		1.1×10^{-4}	[24,29,30]
[Os(NH$_3$)$_5$(DTDPH)]$^{4+}$	−0.73	328		1.1×10^{-4}	[24,29,30]
[Os(NH$_3$)$_5$(DTDPH)]$^{3+}$		488		8.5×10^3	[24,29]
[Os(NH$_3$)$_5$py]$^{3+}$	−0.64	266, 290		$4.3 \times 10^3, 2.5 \times 10^3$	[39]

[a] Volts, versus SCE at 25°C, $\mu = 0.10$ M, expressed with two significant figures.
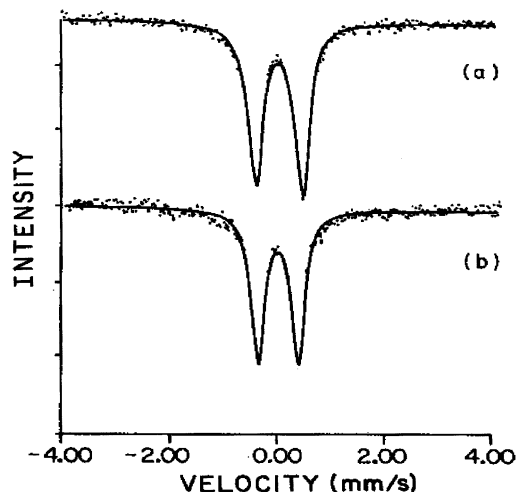
Fig. 2. Mössbauer spectra [27] of the mixed valence complexes (a) $[(CN)_5Fe^{II}(DTDP)Ru^{III}(NH_3)_5]$ and (b) $[(CN)_5Fe^{II}(DTDP)Fe^{III}(CN)_5]$.

4. Binuclear and trinuclear complexes

4.1. Mössbauer measurements

Doublets are the main feature in Mössbauer spectra of mononuclear pentacyano complexes due to the presence of an electric field gradient with non-cubic symmetry at the ^{57}Fe nucleus [55]. The non cubic electronic symmetry is a consequence of the asymmetric σ and π bonding along the Z axis, which is responsible for the appearance of the electric field gradient (EFG) at the iron nucleus and consequently for the quadrupole splitting Δ_{Qs}. The isomer shift δ, reflects the changes in the electronic density at the nucleus due to the electron population modifications of valence orbitals of the Mössbauer atom.

The iron nucleus is less shielded in Fe(III)—DTDP species (d^5 low spin) than in Fe(II)—DTDP complexes (d^6 low-spin). However Fe(III) complexes exhibit bigger EFG than the counterpart Fe(II) ions due to the asymmetric electronic configuration. As a consequence for Fe(III) species, the values for δ are expected to be much smaller and Δ_{Qs} much bigger than those observed for the analogous Fe(II) complexes, see Table 3.

There is no evidence for Fe(III) or Fe(II) quadrupole splitting in the Mössbauer spectra of the homobinuclear and of the heterobinuclear mixed valence complexes, (as illustrated in Fig. 2 for the $Na_5[(CN)_5Fe(DTDP)Fe(CN)_5]5·H_2O$ species), therefore suggesting an electron delocalization between the two metal centers [26,27]. However the Mössbauer spectrum of the Fe(II)(BPMS)Fe(III) complex shows [53] two quadrupole splitting patterns suggesting that the $-CH_2-S-S-CH_2-$ bridge, conversely to the $-S-S-$ one, acts as an insulator.

The bigger Δ_{Qs} and smaller δ values observed for the Fe(III)–DTDP–Fe(II) species, compared with those of Fe(II)–DTDP–Fe(II) suggest some degree of electron delocalization between the two iron centers. The isomer shift and the quadrupole splitting values measured for $Na[(CN)_5Fe^{II}(DTDP)Ru^{II}(NH_3)_5]\cdot6H_2O$ are very close to the ones found for the monomer $Na_3[Fe^{II}(CN)_5(DTDP)]\cdot4H_2O$. The smallest isomer shift observed for the heterobinuclear mixed valence species, relative to the fully reduced parent complex, is consistent with the presence of the good Lewis acid Ru(III), which will stabilize the DTDP π^* orbitals leading to an increase in the $d_\pi[(CN)_5Fe^{II}] \rightarrow p\pi^*$ DTDP interaction.

Increase in the extension of the Fe(II) $\rightarrow$ DTDP back-bonding leads to a decrease in the Fe(II) t_{2g} orbital population, thus a deshielding in the s orbitals, which will contribute to a decrease in the δ value. This effect correlates with the observed increase in the Δ_{Qs} value for the mixed valence heterobinuclear species.

The shape of the Mössbauer spectrum depends on the relative rate of Mössbauer nuclear excited state decay k_n, compared to the rate of intervalence electron transfer k_e. Thus, despite the fact that evidence exists for electron delocalization through the –S–S– bridge, more data is required before definitive conclusions and assignments on these systems can be drawn.

5. Near-infrared and comproportionation constant data

The relevant characteristics of binuclear complexes in which the bridging ligands are DTDP [22,23,26–29] or BPMS [53] are presented in Tables 4 and 5.

The homobinuclear species in the fully reduced form exhibit intense metal-to-ligand (MLCT) bands and in the same energy range as the parent mononuclear complexes. The oxidation of one metal center in these complexes leads to a decrease in the MLCT band intensity.

The main change is observed in the near-infrared (NIR) region of the mixed valence homobinuclear DTDP complex spectra. For the (II,III) species [22,23,26,29] an intervalence band (MMTC) is observed, which in its form, energy and intensity clearly indicate considerable [56] electron delocalization between the two metal

Table 4
Mössbauer parameter data[a] at 300 K using nitroprusside as reference

Complexes	$\delta \pm 10^{-4}$ (nm s^{-1})	$\Delta_{Qs} \pm 10^{-3}$ (nm s^{-1})
$Na_3[Fe^{II}(CN)_5(DTDP)]\cdot4H_2O$	0.291	0.886
$Na_2[Fe^{III}(CN)_5(DTDP)\cdot4H_2O$	0.220	1.709
$Na_5[(CN)_5Fe^{II}(DTDP)Fe^{III}(CN)_5]\cdot5H_2O$	0.278	0.740
$Na_6[(CN)_5Fe^{II}(DTDP)Fe^{II}(CN)_5]\cdot6H_2O$	0.300	0.705
$Na[(CN)_5)Fe^{II}(DTDP)Ru^{II}(NH_3)_5]\cdot6H_2O$	0.293	0.887
$[(CN)_5Fe^{III}(DTDP)Ru^{III}(NH_3)_5]\cdot5H_2O$	0.275	0.910

[a] Adapted from Refs. [26,27].

Table 5
Absorption data and reduction potentials for mono and heterobinuclear complexes

Species	MLCT (cm^{-1})[a]	ε $(M^{-1} cm^{-1})$ $\times 10^{-3}$	MMCT (cm^{-1})[a]	ε $(M^{-1} cm^{-1})$ $\times 10^{-3}$	$\Delta(\nu_{1/2})$ $(M^{-1} cm^{-1})$ $\times 10^{-3}$	E_i[b]	E_2[b]	Ref.
$[(NH_3)_5Os(DTDP)Fe(CN)_5]$	435		790		7.7	-726	32	[28–30]
$[(NH_3)_5Ru(DTDP)Fe(CN)_5]$	416		1250			93	289	[27,29]
$[(NH_3)_5Ru(DTDP)Fe(CN)_5]$	458	5.0						[27,29]
$[(NH_3)_5Ru(DTDP)]Ru(CN)_5]$	360					95	710	[22,23]
$[(NH_3)_5Ru(DTDP)Ru(CN)_5]^-$	462	7.0						[23]
$[(NH_3)_5Ru(DTDP)Os(NH_3)_5]^{5+}$	464	965	2.16	3.3		-550	140	27,29
$[(NH_3)_5Ru(DTDP)Ru(NH_3)_5]^{5+}$	468	15	1500	4.26	12.4			[22,23]
$[(NH_3)_5Ru(DTDP)Ru(NH_3)_5]^{4+}$	466	19				-130	160	[22,23]
$[(NH_3)_5Ru(BPMS)Ru(NH_3)_5]^{4+}$	426	4.9					95	[52]
$[(CN)_5Fe(DTDP)Fe(CN)_5]^{5-}$	408	7.1	1195	0.90	4.02			[22,23]
$[(CN)_5Fe(DTDP)Fe(CN)_5]^{6-}$	412	9.3				155	275	[22,23]
$[(CN)_5Fe(BPMS)Fe(CN)_5]^{6-}$	394	7.8					240	[53]
$[(NH_3)_5Os(DTDP)]^{3+}$	312					-590		[24]
$[(NH_3)_5Ru(DTDP)]^{2+}$	458						95	[22,23]
$[(CN)_5Ru(DTDP)]^{3-}$	348						710	[23]
$[(CN)_5Fe(DTDP)]^{3-}$	412						255	[23]
$[(NH_3)_5Ru(BPMS)]^{2+}$	422	2.5					54	[53]
$[(CN)_5Fe(BPMS)]^{3-}$	394	4.1					233	[53]

[a] Uncertainty of ± 2 nm for MLCT, ± 5 nm for MMCT.
[b] $(E^{\circ\prime}_{1/2})$ mV versus SCE for M(III)/M(II) couple.

centers. The characteristics of this intervalence band for the ruthenium species are: $\lambda_{max} = 1.500$ cm^{-1}; $\varepsilon = 4.3 \times 10^3$ M^{-1} cm^{-1}; bandwith at half intensity ($\Delta v_{1/2}$) = 1.24×10^3 cm^{-1} (Calc. = 3.92×10^3) [56–59] and electronic coupling (H_{AB}) = 855 cm^{-1}. For [(CN)$_5$Fe(DTDP)Fe(CN)$_5$]$^{5-}$, the MMTC band is centered at $\lambda_{max} =$ 1195 mm, $\varepsilon = 9.0 \times 10^3$ M^{-1} (Calc. = 4.4×10^3) and $H_{AB} = 466$cm^{-1}. The energetic barrier (ΔG_{th}) [57–59] estimated on the basis of the energy (E_{op}) of the intervalence band is 4.7 and 5.9 kcal mol^{-1} for the ruthenium and the iron species, respectively. These energies are of the same order of magnitude as the value calculated [57,58] for the Creutz–Taube ion: 5.6 kcal mol^{-1}.

No NIR band could be observed in the spectra of the [(CN)$_5$Fe(BPMS)Fe(CN)$_5$]$^{5-}$ and [(NH$_3$)$_5$Ru(BPMS)Ru(NH$_3$)$_5$]$^{5+}$ species [53]. This observation is in agreement with Mössbauer data [27,53] and strongly suggests that BPMS, in contrast with DTDP, does not promote any significant electron delocalization between the two metal centers.

Metal-to-ligand charge transfer bands are always present in the spectra of the heterobinuclear complexes. An inspection of the data in Table 5 [22,23,27,28] will suggest that the contribution of the [Ru(NH$_3$)$_5$]$^{2+}$ moiety is dominant in the MLCT band present in the spectra of [(NH$_3$)$_5$Ru(DTDP)Ru(CN)$_5$]$^-$, [(NH$_3$)$_5$Ru(DTDP)Fe(CN)$_5$]$^-$ and [(NH$_3$)$_5$Ru(DTDP)Os(NH$_3$)$_5$]$^{5+}$ species. For the mixed valence species [(NH$_3$)$_5$Ru(DTDP)Ru(CN)$_5$], [(NH$_3$)$_5$Ru(DTDP)Fe(CN)$_5$] and [(NH$_3$)$_5$Os-(DTDP)Fe(CN)$_5$] the fragment [M(CN)$_5$]$^{3-}$ is the main one responsible for the MLCT absorption.

Along with the efficiency of the –S–S– bridge as a conductor, for all the heterobinuclear mixed valence species, the energy of the MLCT band is intermediate between the energies of the charge transfer bands of its monomers.

In heterobinuclear mixed valence species spectra a low energy band $\lambda_{max} > 790$ nm could be detected. This band which is absent in the monomers and in the
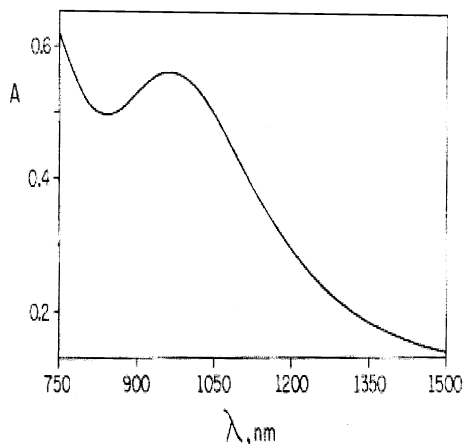
Fig. 3. NIR spectrum for the mixed valence [(NH$_3$)$_5$Os(DTDP)Ru(NH$_3$)$_5$]$^{5+}$ ion; $C = 2.6 \times 10^{-3}$ M, in D$_2$O.

Table 6
NIR data[a] and comproportionation constants for homobinuclear metal complexes
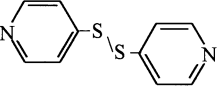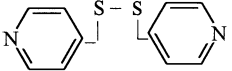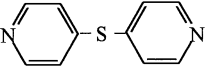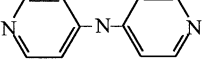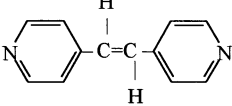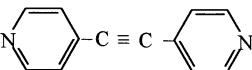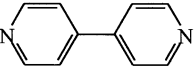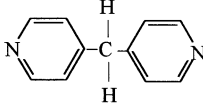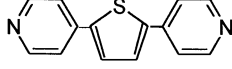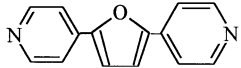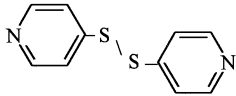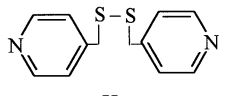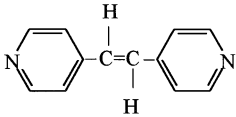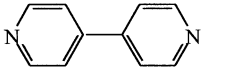
Metal Systems	L	NIR Bands		K_c [b]
		λ_{max}(nm)	ε (M^{-1}cm^{-1})	
$[(NH_3)_5 Ru]_2 L$		1570	5000	4×10^6
		1500	4260	8×10^4
				< 10
		855	70	<10
		920	1010	5×10^2
		960	760	
		920	640	14
		1030	920	2×10
		810	30	9.8
		985	410	14[c]
		992	520	50[c]
$[(CN)_5 Fe]_2 L$		1200	2200	5×10^2

Table 6 (*Continued*)

Structure			
(pyridyl–S–S–pyridyl)	1195	900	1×10^2
(pyridyl–S–S–pyridyl with L marks)			$<10^b$
(pyridyl–CH=CH–pyridyl, H above and below)	1300	600	<10
(bipyridyl)	1200	1100	<10

a) Adapted from refs.5, 23 and 26.

b) K_c is equal to exp ($\Delta E_{1/2}/25.68$), T = 298K, $n_1 = n_2 = 1$.

c) ref. 61

binuclear fully oxidized or reduced species spectra was attributed to an MMCT transition [27].

For $[(NH_3)_5Os(DTDP)Ru(NH_3)_5]^{5+}$ ions, (see Fig. 3) it was possible to calculate [58–60] $H_{AB} = 2.2 \times 10^2$ cm^{-1} and the electronic delocalization parameter α as 4×10^4, by taking the calculated [43] average distance between the two metal centers as 8.2 Å,

Some other useful information about the mediator ability of the ligand bridging two metal centers at different oxidation states M^{II}–L–M^{III}, was obtained from the comproportionation constant K_c [55–59], for the reaction:

$$[II, II] + [II] \overset{K_c}{\rightleftharpoons} 2[III, II]$$
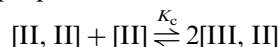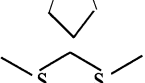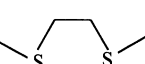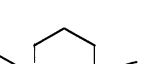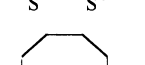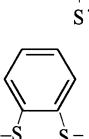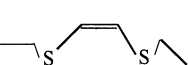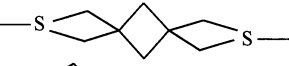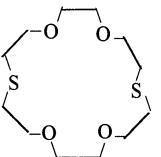
From the voltammograms of $[(NH_3)_5Ru(DTDP)Ru(NH_3)_5]^{4+}$ and $[(CN)_5Fe(DTDP)Fe(CN)_5]^{6-}$ species it was possible to calculate the comproportionation constants of 8×10^4 and 1×10^2. For the BPMS [54] and DPS [9] analogues, the calculated K_c values are smaller than 10.

It is interesting to point out that the –S–S– bridge, in DTDP complexes, provides more electron delocalization [9,23,58–61] than NH, methylene, ethylene, acetylene, thiophene and furan groups, (see Table 6).

A comparison of the efficiency of bidentate sulfur ligands can be seen in Table 7. In these ligands [10–13], the sulfur atoms lie apart from one another and since only a σ-bonded framework is involved, the bridge mediation effects have been explained either based on sulfur–sulfur through space interaction [10,13] for the small ligands or assuming some electron tunneling for the spiro-ring type ligands [62–64].

Table 7

NIR bands and comproportionation constants for binuclear ruthenium(II,III) mixed-valence compounds, $[(NH_3)_5Ru^{II}-L-Ru^{III}(NH_3)_5]^{5+}$

L	NIR Bands		K_c
	λ_{max}(nm)	ε (M^{-1} cm^{-1})	
	1220	86	892
	1000	64	~185
	996	55	~100
	972	6	~40
	1210	80	<10
	928	45	125
	840	21	<10
	775	5	<10
	615	0.75	<10
	1132	35	~48
	964	22	~30
	910	43	<10
	808	9	
	690	2.3 ± 0.7	
	860	3	<10
—S—S— [b]	647		8×10^{16}

a) Data are adapted from ref. 5, 23 and 26; b) ref. 80.

For DTDP mixed valence complexes, the two pyridine rings, (each one coordinated to a charged metal center), will be separated to minimize electrostatic interactions. Thus, through-space interactions are unlikely to occur in the DTDP binuclear complexes.

It is remarkable that BPMS [54] and DPS [9], being ligands which closely resemble the DTDP species do not exhibit conductor properties. These two systems, could be regarded as a DTDP ligand where one CH_2 group was introduced into each side of the –S–S– bridge (BPMS) or a sulfur atom abstracted (DPS). In both cases, the coupling between the two metal centers is so weak that only one redox process can be observed [9,54] in their voltammetric spectra.

The investigations have been extended [28,29] to the trinuclear complex ion $[(NH_3)_5Ru(DTDP)Ru(NH_3)_4(DTDP)Ru(NH_3)_5]^{6+}$. This trinuclear species exhibits an MLCT band at 462 nm ($\varepsilon = (2.0 \pm 0.1) \times 10^4$ M^{-1} cm^{-1}) and two redox processes (see Fig. 4), with the area of the peak at $(E^{\circ\prime}_{1/2})_1 = 0.090$ V being twice that at $(E^{\circ\prime}_{1/2})_2 = 0.30$ V.

The central ruthenium ion bound to two DTDP ligands is more resistant to oxidation than the two other terminal ruthenium centers, as indicated by $E^{\circ\prime}_{M(III)/M(II)}$ for the $[(NH_3)_5Ru(DTDP)]^{3+/2+}$ and *trans*-$[(NH_3)_4Ru(DTDP)_2]^{3+/2+}$ in Table 3. A careful deconvolution analysis of the peak at $(E^{\circ\prime}_{1/2})_1 = 0.090$ V allows the separation of this process into two components in which $(\Delta E_{1/2}) \cong 20$ mV, see Fig. 4.

The calculated [28,29] comproportionation constant K_c, for the reaction.

$$[III, II, III] + [II, II, II] = 2[III, II, II]$$
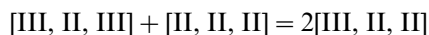
barely exceeds the statistical value of 4, suggesting that the end-to-end communication is very weak. The absence of any band attributed to an MMCT transition in the NIR spectrum of [III, II, II] species provides additional support to the above conclusion.

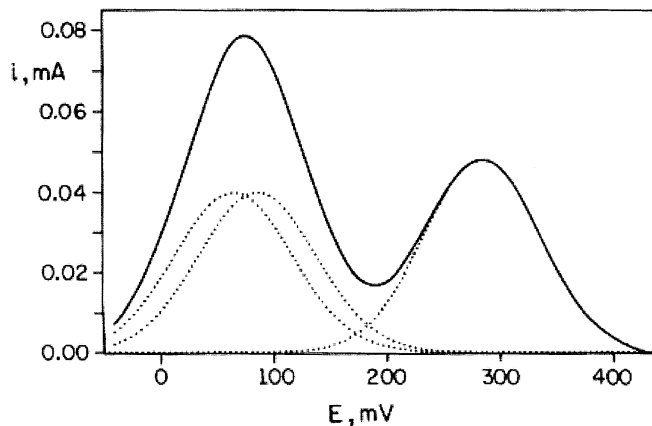Fig. 4. Differential pulse polarogram for *trans*-$[(NH_3)_5Ru(DTDP)Ru(NH_3)_4(DTP)Ru(NH_3)_5]^{6+}$, $\mu = 0.10$ M (NaCF$_3$COO/HCF$_3$COO), CF$_3$COOH $= 1.0 \times 10^{-3}$ M; $C_{complex} = 1.0 \times 10^{-3}$ M, 25°C, E versus the saturated calomel electrode (SCE).

The calculated K_c value [65] of 70 for $[(NH_3)_5Ru(pz)Ru(NH_3)_4(pz)Ru(NH_3)_5]^{7+/6+}$ system is significantly higher than the one calculated for the parent DTDP analogue.

Electronic repulsions due to the back-bonding into a common orbital from two metal centers were invoked to explain the large value of Creutz-Taube [57–59] ion comproportionation constant, 4×10^6. In the trinuclear species, when the terminal ruthenium centers are linked by the *trans*-tetraammineruthenium unit, these repulsions are less intense and a smaller comproportionation constant for the [II, II, II] species in comparison to [II, II] is expected. Furthermore the electronic factor Δ, which is directly proportional to electron delocalization and is larger [66] for pz than for DTDP, should decrease with the increase in distance between the two metal centers [59,66]. These effects would be more evident when DTDP is the bridging ligand and the end-to-end communication distance [43] is ~ 16 Å.

At this point some comments on the relevance of the bonding character in the –S–S– bridge properties seem in order. There is evidence of p_π–d_π overlap in aromatic disulfides, which have sulfur atoms directly bound to aromatic rings. In these systems the sulfur–sulfur distances are shorter than expected [67–72], for a pure single bond, and the L–S–S–L dihedral angle is very close to 90°. This condition maximizes π overlap between the 3pπ orbitals of two neighboring S atoms and minimizes, due to the orthogonality of the orbitals, the sulfur atom lone-pair repulsion [69–73].

In DTDP the S–S bond length [67] is 2.03 Å and the dihedral angle is 80.3°. The S–S bond is nearly in the plane of each pyridine ring. Strong interactions between the π orbitals of the pyridine rings (filled pπ, empty pπ*) and π orbitals of the sulfur atoms (half filled 3pπ, empty 3dπ) have been a matter of discussion [67–74].

In the mono and binuclear complexes, the DTDP ligand, the coordinated pyridine rings and the –S–S– bridge lie in the same plane exhibiting a *trans* planar structure similar to the one observed for the Ru–S–S–Ru moiety in related complexes [4,5,62,69,72,75–78]:
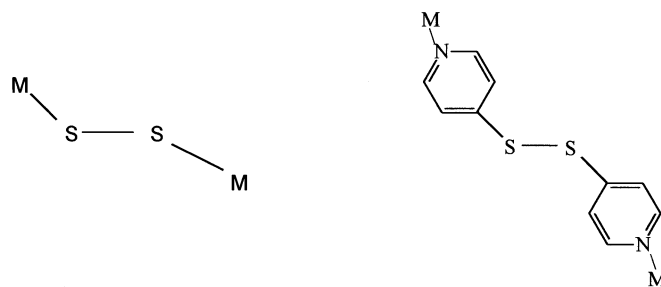
M = Fe, Ru, Os

In this configuration the filled π orbitals of the coordinated pyridine rings (or one of the t_{2g}^6 orbitals of each metal center in the Ru_2S_2 core) would have the appropriate [72–74,78] symmetry and orientation for π interaction with the orbitals of the S_2^- ligand. Deviations from this *trans*-butadiene like π network [76–78]

would diminish the degree of π bonding and therefore the delocalization along the L⋯S⋯S⋯L core, (L = M or py).

In the BPMS ligand CH_2 groups are located between the pyridine rings and the sulfur bridge, and in the DPS only one sulfur atom exists between the pyridine rings. Thus, in the complexes of both of these ligands the structures L–CH_2–S–S–CH_2–L and L–S–L were not of the *trans* planar type, therefore not fulfilling the above requirements for electron delocalization [76–78]. Unfortunately crystal structure data for BPMS and DPS, which will certainly shed more light on this subject, are not yet available.

The coordination to metal centers and the presence of solvent molecules will induce changes in the DTDP ligand structrure relative to the crystal. Even so it is likely that in this framework communication between the two pyridine rings, through π orbitals of the C–S–S–C backbone, is more favorable to occur than in BPMS and DPS.

In transition metal complexes the participation of orbitals other than those often used in the $nd_\pi \rightarrow 3d_\pi$ back-bonding interaction was discussed [71,72] At least in systems in which sulfur atoms were bonded to carbon atoms and a nodal plane at the binding site precludes back-bonding interactions, σ* orbitals derived from atomic 2p on C and 3p on S were considered [65,62,72].

The μ-S_2 complexes are particularly atractive since the donor and the acceptor atoms are directly bonded to the S_2^- unit. The π-bond interaction across the RuSSRu core, whose Ru–S–S–R dihedral angle is 180°, was suggested by the shorter Ru–S (2.193 Å) and S–S (2.014 Å) distances [69,75] in [$(NH_3)_5$RuSSRu-$(NH_3)_5$]$Cl_4 \cdot 2H_2O$ than those calculated [69,75,76] by the sum of single-bond radii. In this case, two occupied ruthenium d_π orbitals and the occupied π as well as the empty π* orbital of the S–S bridge combine to give one empty π_4 (LUMO) and three occupied molecular orbitals π_3 (HOMO), π_2 and π_1.

The Ru–S–S–Ru moiety, to which the formulation Ru^{II}–(S_2^-)–Ru^{III} was proposed [69,72c,d] is considered the chromophore responsible for the green color exhibited by [$(NH_3)_4$LRuSSRu$(NH_3)_4$L]$^{n+}$, (when L = Cl$^-$, Br$^-$, I$^-$, n = 4. L = isn and NH_3, n = 4. L = NO$^+$, n = 6) and other non ammine species [72c,73,76,78]. For all these complexes except [$(\mu$-$S_2)\{Ru(PPh_3)'S_4'\}_2$], the $\pi_3 \rightarrow \pi_4$ HOMO–LUMO transition occurs in the 600–800 nm range. The energy of this $\pi_3 \rightarrow \pi_4$ transition is sensitive to the ruthenium centers coordination sphere composition. In [$(\mu$-$S_2)\{Ru(PPh_3)'S_4'\}_2$], the $\pi_3 \rightarrow \pi_4$ transition was assigned at 1049 cm^{-1}, $\varepsilon = 1.3 \times 10^4$ M^{-1} cm^{-1}), being the absorption responsable for the 'green color' (645 nm, $\varepsilon = 8.9 \times 10^3$ M^{-1} cm^{-1}) attributed to the $\pi_2 \rightarrow \pi_4$ transition [78]. No MMCT transition was identified in the spectra of the above mentioned species.

Unfortunately the instability of the $Ru^{III}SSRu^{II}$ core in [L$(NH_3)_4$-RuSSRu$(NH_3)_4$L]$^{n+}$ complexes has prevented [3–5,8] reliable direct measurements (E°$_{1/2}$, NIR) of the S_2^{2-} bridge efficiency as an electron conductor. Recently, the [$(CH_3CN)_3(P(OMe)_3)_2$RuSSRu$(P(OMe)_3)_2(CH_3CN)_3$]$^{2+/3+/4+}$ system has been described [79]. In the [II, III] species the measured Ru–S and S–S distances are 2.322 and 1.995 Å, respectively, and K_c has the remarkable value of 8.0×10^{16}. Due to the strong π delocalization through the S_2^{2-} ligand, the NIR band in these [II, III]

species was [79] strongly coupled, and therefore mixed, with the LMCT band at 647 nm.

These new observations [79], with technological implications in material science [78–82] will be an additional incentive to the study of the S–S bridge properties. Efforts [43] are being made to obtain reliable quantum mechanical calculations and X-ray crystallographic data for selected systems with the aim of access to information, which would better describe the –S–S– bridge behavior.

Acknowledgements

References

[1] J. Taube, Surv. Prog. Chem. 6 (1973) 1.
[2] P.C. Ford, Coord. Chem. Rev. 5 (1970) 75.
[3] C.G. Kuehn, H. Taube, J. Am. Chem. Soc. 98 (1976) 689.
[4] C.R. Brulet, S.S. Isied, H. Taube, J. Am. Chem. Soc. 95 (1973) 4758.
[5] C.G. Kuehn, S.S. Isied, Prog. Inorg. Chem. 27 (1980) 1048.
[6] S.S. Isied, H. Taube, J. Am. Chem. Soc. 95 (1973) 8198.
[7] S.S. Isied, H. Taube, Inorg. Chem. 13 (1974) 1545.
[8] S.S. Isied, Ph.D. Dissertation, Stanford University, USA, 1973.
[9] H. Fischer, G.M. Tom, H. Taube, J. Am. Chem. Soc. 98 (1976) 5512.
[10] C.A. Stein, H. Taube, J. Am. Chem. Soc. 100 (1978) 1635.
[11] C.A. Stein, H. Taube, Inorg. Chem. 18 (1979) 1168.
[12] C.A. Stein, H. Taube, Inorg. Chem. 18 (1979) 2212.
[13] C.A. Stein, H. Taube, J. Am. Chem. Soc. 103 (1981) 693.
[14] D.P. Fairlie, W.A. Wickramesinghe, K.A. Bynel, H. Taube, Inorg. Chem. 36 (1997) 2242.
[15] H. Taube, Pure Appl. Chem. 511 (1979) 901.
[16] H. Taube, Comments Inorg. Chem. 17 (1981) 1.
[17] (a) M.T. Stankovich, A.J. Bard, J. Electroanal. Chem. 75 (1977) 487. (b) E.I. Steifel, K. Matsumoto, Transition Metal Sulfur Chemistry, Biological and Industrial Significance, American Chemistry Society, Washington, DC, 1996.
[18] (a) J. Daí, M. Munakata, L.-P Wu, T. Kurosa-Sowa, Y. Suenaga, Inorg. Chim. Acta 258 (1997) 65. (b) A. Heller, Acc. Chem. Res. 23 (1990) 128.
[19] (a) T.G. Harvey, T.W. Matheson, J. Chem. Soc. Chem. Commun. (1985) 188. (b) R.H. Holm, D.E. Simhon, in: T.G. Spiro (Ed.), Molybdenum Enzimes, Wiley Interscience, New York, 1985 (Chapter 1).
[20] (a) T. Ishirguro, K. Yamaji, Organic Super-Conductors, Springer, Berlin, 1990. (b) B. Pomarede, B. Garreau, I. Malfant, L. Valade, P. Cassoux, J.-P. Legros, A. Audouard, L. Brossard, J.-P. Ulmet, M.-L. Doublet, E. Canadell, Inorg. Chem. 33 (1994) 3401.

[21] (a) G. Pistoia (Ed.), Lithium Batteries New Materials, Developments, Perspectives, Elsevier, New York, 1994. (b) H. Ezzovia, R. Reindl, R. Parsons, H. Tributsch, J. Electronal. Chem. Interfacial Electrochem. 165 (1984) 155.
[22] I.S. Moreira, D.W. Franco, J. Chem. Soc. Commun. 5 (1992) 450.
[23] I.S. Moreira, D.W. Franco, Inorg. Chem. 33 (1994) 1607.
[24] J.B. Lima, A.N. Medina, F.G. Gandra, D.W. Franco, Proceedings of the 30th International Conference on Coordination Chemistry, Kyoto, Japan, 1994, pp. 2–152.
[25] A.N. Medina, F.G. Gandra, L.M. Baesso, J.B. Lima, B.R. McGarvey, D.W. Franco, J. Chem. Soc. Faraday Trans. 93 (1997) 2105.
[26] I.S. Moreira and D.W. Franco, in: S.S. Isied (Ed.), Electron Delocalization through the Disulfide Bridge, Advances in Chemistry 253, American Chemical Society, Washington, DC, 1997 (Chapter 15).
[27] I.S. Moreira, E.C. Lima, D.W. Franco, Inorg. Chim. Acta 267 (1998) 93.
[28] J.B. Lima, D.W. Franco, in preparation.
[29] J.B. Lima, Ph.D. Dissertation, Instituto de Química de São Carlos, USP, Brazil, 1996.
[30] W.C. Silva, M.S. Dissertation, Universidade Federal do Ceará, UFC, Brazil, 1999.
[31] L.A. Marinho and D.W. Franco, unpublished results.
[32] R.E. Shepherd, H. Taube, Inorg. Chem. 12 (1973) 1392.
[33] (a) B.R. McGarvey, Química Nova 21 (1998) 206. (b). B.R. McGarvey, Coord. Chem. Rev. 170 (1998) 75.
[34] K.J. Lachance-Galang, P.E. Doan, M.J. Clarke, U. Rao, A. Yamano, B.M. Hoffman, J. Am. Chem. Soc. 117 (1995) 3529.
[35] P.A. Lay, D.W. Harman, Adv. Inorg. Chem. 37 (1991) 219.
[36] P.A. Lay, R.H. Magnuson, H. Taube, J. Ferguson, E.R. Krausz, Inorg. Chem. 107 (1985) 2551.
[37] P.A. Lay, R.H. Magnuson, H. Taube, Inorg. Chem. 28 (1989) 2001.
[38] P.C. Ford, F.P. Rudd, R. Gaunder, H. Taube, J. Am. Chem. Soc. 90 (1968) 1187.
[39] J. Sen, H. Taube, Acta Chem. Scand. (1979) 33.
[40] H.E. Toma, E. Staddler, Inorg. Chem. 24 (1985) 3085.
[41] C.R. Jonhson, R.E. Shepherd, Inorg. Chem. 22 (1983) 2439.
[42] S. Zhang, R.E. Shepherd, Transit. Met. Chem. 17 (1992) 199.
[43] J.B.L. Martins, J.B. Lima, E. Longo, D.W. Franco, in preparation.
[44] I.S. Moreira, L.T.S. Parente, D.W. Franco, Quím. Nova 21 (1998) 545.
[45] C. Shi, F.C. Anson, Inorg. Chem. 36 (1997) 2682.
[46] W.W. Henderson, R.E. Shepherd, Inorg. Chem. 24 (1985) 2398.
[47] H.E. Toma, C. Creutz, Inorg. Chem. 16 (1977) 545.
[48] J.F. Ireland, P.A.H. Wyatt, Adv. Phys. Chem. 12 (1967) 131.
[49] A.B.P. Lever, Inorganic Electronic Spectroscopy, second ed., Elsevier, New York, 1984.
[50] H.B. Gray, N.A. Beach, J. Am. Chem. Soc. 85 (1963) 2922.
[51] J.P. Sen, Ph.D. Dissertation, Stanford University, USA, 1969.
[52] C. Creutz, M.D. Newton, N. Sutin, J. Photochem. Photobiol. A Chem. 82 (1994) 47.
[53] M.V. Hrepic, J. Malin, Inorg. Chem. 18 (1979) 409.
[54] E.C. Lima, M.S. Dissertation, Universidade Federal do Ceará, Fortaleza, Brazil, 1995.
[55] D.K. Lavalle, E.B. Fleisher, J. Am. Chem. Soc. (1994) 2583.
[56] A.L. Coelho, I.S. Moreira, J.H. Araújo, M.A.B. Araujo, Radional. Chem. Lett. 136 (1989) 299.
[57] N.S. Hush, Prog. Inorg. Chem. 8 (1967) 391.
[58] H. Taube, Ann. N.Y. Acad. Sci. 313 (1978) 481.
[59] C. Creutz, Prog. Inorg. Chem. 30 (1983) 1.
[60] N.S. Hush, Coord. Chem. Rev. 64 (1985) 135.
[61] A-C. Ribou, J.-P. Launay, K. Takahashi, N. Nihira, S. Tarutani, C.W. Spangler, Inorg. Chem. 33 (1994) 1325.
[62] C.A. Stein, PhD Thesis, Stanford University, USA, 1978.
[63] C.A. Stein, N.A. Lewis, G. Seitz, J. Am. Chem. Soc. 104 (1997) 2242.
[64] N.A. Lewis, S.Y. Obeng, D.V. Taveras, R.V. Eldik, J. Am. Chem. Soc. 111 (1989) 924.
[65] A. von Kameke, G.M. Tom, H. Taube, Inorg. Chem. 17 (1978) 1790.

[66] (a) A. Broo, S. Larson, Chem. Phys. 161 (1992) 363. (b) S. Larson, M. Braga, Chem. Phys. 173 (1993) 367. (c) M.L. Naklicki, C.A.White, L.L. Plante C.E.B. Evans, R.J. Crutchley, Inorg. Chem. 37 (1998) 1880.

[67] J.D. Lee, M.W.R. Bryant, Acta Crystallogr. B 25 (1969) 2094.

[68] N.V. Raghavan, S. Seff, Acta Crystallogr. B 33 (1977) 386.

[69] R.C. Elder, N. Trkula, Inorg. Chem. 16 (1977) 1048.

[70] R.R. Fraser, G. Boussard, J.K. Saunders, J.B. Lambert, C. Mixan, J. Am. Chem. Soc. 93 (1971) 3822.

[71] R. Singh, G.M. Whitesides, J. Am. Chem. Soc. 112 (1990) 6304.

[72] (a) R. Steudel, Angew Chem. Int. Ed. Engl. 14 (1975) 655. (b) M. Herberhold, D. Reiner, U. Thewalt, Angew Chem. Int. Ed. Engl. 22 (1983) 1000. (c) A. Müller, E. Diemann, Sulfides, in: G. Wilkson (Ed.), Comprehensive Coordination Chemistry, vol. 2, Oxford, Pergamon Press, 1987, pp. 515–550. (d) M.G. Gomes, C.U. Davanzo, S.C. Silva, L.G.F. Lopes, P.S. Santos, D.W. Franco, J. Chem. Soc. Dalton Trans. (1998) 601.

[73] J.-H. Chou, T.B. Rauchfuss, L.F. Szczepura, J. Am. Chem. Soc. 120 (1998) 1805.

[74] (a) A. Streitweiser, Jr., S.P. Ewing, J. Am. Chem. Soc. 97 (1975) 97. (b) A. Streitweiser, Jr., J.G. Williams, J. Am. Chem. Soc. 97 (1975) 191. (c) N.H. Epitotis, R.L. Yates, F. Bernardi, S. Wolfe, J. Am. Chem. Soc. 98 (1975) 5435. (d) S. Wolfe, A. Rank, I.G. Csizmodia, J. Am. Chem. Soc. 89 (1967) 89.

[75] S. Kim, E.S. Otterbem, R.P. Rava, S.S. Isied, J.J. Fillipp Jr., J.V.J. Waszcyak, J. Am. Chem. Soc. 105 (1983) 336.

[76] D. Sellmann, P. Lechner, F. Knoch, M. Moll, J. Am. Chem. Soc. 114 (1992) 922.

[77] R. Steudel, Y. Drozdova, K. Miaskiewicz, R.H. Hertwing, W. Koch, J. Am. Chem. Soc. 119 (1997) 1990.

[78] J. Amarasekera, T.B. Rauchfuss, S.R. Wilson, Inorg. Chem. 26 (1987) 3328.

[79] K. Matsumoto, T. Matsumoto, M. Kawano, H. Ohnuki, Y. Shichi, T. Nishide, T. Sato, J. Am. Chem. Soc. 118 (1996) 3597.

[80] T.N. Lockyer, R.L. Martin, Prog. Inorg. Chem. 27 (1979) 223.

[81] J.M. Williams, Prog. Inorg. Chem. 33 (1985) 183.

[82] A.R. Armstrong, P.G. Bruce, Nature 381 (1996) 499.